JOURNAL OF AGRICULTURAL AND FOOD CHEMISTRY

ARTICLE

pubs.acs.org/JAFC

Effect of Starch on the Molecular Mobility of Amorphous Sucrose

Yumin You and Richard D. Ludescher*

Department of Food Science, Rutgers, The State University of New Jersey, 65 Dudley Road, New Brunswick, New Jersey 08901-8520, United States

ABSTRACT: Molecular mobility in amorphous solid biomaterials is modulated by the composition and environment (primarily temperature). Phosphorescence of the triplet probe erythrosin B was used to generate a mobility map within amorphous sucrose films doped with starch ranging from 0.001 to 0.1 g starch/g sucrose. Data on the emission energy and lifetime of erythrosin B in sucrose and sucrose−starch films over the temperature range from 5 to 100 °C indicates that starch influences the molecular mobility as well as dynamic site heterogeneity of amorphous sucrose in a dose-dependent manner. At a starch/sucrose weight (wt) ratio below 0.005, both emission energy and lifetime decreased, and both the dipolar relaxation rate and nonradiative quenching rate k_{TS0} increased, indicating that starch increased the matrix molecular mobility. At a ratio above 0.005, both emission energy and lifetime increased, and the dipolar relaxation rate and nonradiative quenching rate decreased, indicating that starch decreased the matrix mobility both in the glass and in the melt. The mobility showed a minimum value at a ratio of 0.01. The interactions existing in the sucrose−starch matrix are considered as the determining factor to influence the molecular mobility of sucrose−starch mixtures. Changes in the distribution of emission energies (emission bandwidth) and lifetimes indicated that starch increased the spectral heterogeneity at high contents while showing insignificant change or a slight decrease in the heterogeneity at low starch contents. These data illustrate the complex effects of a polymer with mainly linear structure and flexible conformation on the mobility of an amorphous, hydrogen bonded sugar matrix.

KEYWORDS: Sugar glass, amorphous solid, phosphorescence, molecular mobility

INTRODUCTION

Sucrose glasses stabilize plants and other organisms during anhydrobiosis, protect biomaterials from freeze−thaw damage, and provide long-term stability during storage for labile vitamins and flavor compounds in foods, for drugs, and other bioactives in pharmaceuticals, and for enzymes, antibodies, and other proteins.

Two main mechanisms, glass dynamics and specific interaction, have been proposed to understand the role of sugars in stabilizing sensitive compounds during dehydration and storage.[1,2] The glass dynamics mechanism[3] focuses on the rigid, inert matrix formed by the vitrification (glass formation) of stabilizers such as sugars. The specific interaction mechanism,[4] commonly used to explain protein stabilization, focuses on the hydrogen bonds that form at specific sites between amorphous sugars and target compounds, help maintain the native structure and integrity of the molecule (protein) after water is removed, and consequently enhance long-term stability.

Sucrose is considered an excellent matrix material for long-term storage of biomaterials since it is both a good glass former as well as a good hydrogen bond former. However, compared with other disaccharides such as trehalose, sucrose has lower physical stability due to a lower glass transition temperature (T_g). It has been suggested that addition of a polysaccharide to amorphous sucrose will improve its function as a stabilizer.[5]

Starch is a versatile food ingredient and is widely used as a texturizer, thickener, gelling agent, adhesive, and moisture-retainer. Recently, much attention has been focused on the influence of small molecules on the properties of starch, such as the plasticizing effect of water,[6] glycerol,[7] and sorbitol,[8] the anti-plasticizing effect of small molecules,[9] and the effect of sugars on glass transition and molecular mobility in starch-based systems.[10] Few studies, however, have focused on the effect of starch on the properties of sucrose-based systems. Since starch has been suggested to improve the stability of sucrose, measurement of the molecular mobility of a mixed starch−sucrose matrix becomes a pressing issue.

Molecular mobility within amorphous solids is usually manifested by relaxation processes. Amorphous solids exhibit a primary α or glass transition at T_g which reflects the activation of large-scale molecular motions (α-relaxations) that underlie the onset of translational and rotational motion within the matrix; they also exhibit secondary transitions, activated at T_β ($T_\beta < T_g$), which reflect the activation of localized molecular motions (β-relaxations) linked to vibrations and/or side-chain motions within the glass. Temperature-dependent molecular mobility within the amorphous solid controls physical and chemical properties by modulating the nature and kinetics of reactions that occur during processing and storage of biomaterials.

In a previous study, we used erythrosin B phosphorescence to monitor the molecular mobility as well as dynamic site heterogeneity in amorphous solid sucrose.[11] In the present study, phosphorescence of Ery B was used to measure the matrix mobility in thin films of amorphous sucrose−starch mixtures. High-amylose starch was selected because of its ability to form films. The measurement of the molecular mobility of amorphous sugars at low levels of macromolecules provides insight into the mechanism by which the biopolymer affects sucrose matrix mobility, a question of considerable fundamental and

Received: October 27, 2010
Accepted: February 8, 2011
Revised: February 7, 2011
Published: March 07, 2011

dx.doi.org/10.1021/jf1041432 | J. Agric. Food Chem. 2011, 59, 3340–3347

technological interest. Starch content was varied from 0.001 to 0.1 (g starch/g sucrose) by the addition of starch to the concentrated sucrose solution prior to film formation. The temperature dependence of mobility was measured and analyzed at different starch contents, generating families of mobility versus temperature curves.

MATERIALS AND METHODS

Preparation of Sucrose Films. Sucrose was purchased from Sigma-Aldrich (St. Louis, MO) with a minimum purity of 99.5%. Sucrose was further purified using the method described by Pravinata et al.[11]

The free acid of erythrosin B (Ery B, tetra-iodo fluorescein; Sigma Chemical Co., St. Louis, MO) was dissolved in spectrophotometric grade dimethylformamide (DMF; Aldrich Chemical Co., Milwaukee, WI) to prepare a 10 mM stock solution; an aliquot from this solution was added to the concentrated sucrose to obtain a dye/sucrose mole ratio of $1{:}10^4$.

Glassy sucrose films were prepared on quartz slides as described in our previous study.[11] The slides were stored against P_2O_5 and Drie-Rite for at least 7 days and checked for crystals within the film through crossed polarizers in a dissecting microscope (Nikon Type 102, Japan) before any phosphorescence measurements.

Preparation of Starch−Sucrose Films. Corn starch HYLON VII (71% amylose, molecular weight 243,000−972,000) was obtained as a generous gift from National Starch (Bridgewater, NJ) and used without further treatment. Starch−sucrose solutions were prepared from a sucrose solution containing dye. Sufficient water was added to the starch powder to make a slurry with starch concentration less than 3 wt %. The slurry of starch granules was then heated with vigorous stirring on a hot plate to boiling for 30−40 min. The hot starch solution was then mixed thoroughly with prewarmed 64−66% sucrose solution (70 °C) to prepare starch−sucrose mixtures with starch/sucrose weight (wt) ratios of 0.001, 0.0025, 0.005, 0.01, 0.025, 0.05, and 0.1. The final mixtures were checked using a microscope to ensure that starch granules were completely hydrated and gelatinized. After gelatinization, solutions were filtered through a 0.2 μm membrane to remove insoluble granule remnants. The starch−sucrose solutions were kept hot (above 80 °C) before casting films. The procedure to make a glassy starch−sucrose film was the same as the procedure to make a pure sucrose film except for the drying of films for 10 min instead of 5 min.

Water content in amorphous sucrose and sucrose−starch films was determined gravimetrically (by difference of mass before and after drying for 24 h at 70 °C in an Ephortee (Haake Buchler, Inc.) vacuum oven at 1 kPa). Sample films were scrapped from quartz slides and ground into powders in a glovebox containing P_2O_5 and Drie-Rite with a relative humidity less than 5%. Pure sucrose films contained 0.56 ± 0.13 wt % water, while the starch/sucrose mixture samples contained 0.58 ± 0.01, 0.50 ± 0.08, 1.05 ± 0.03, 1.28 ± 0.27, 1.50 ± 0.05, 1.75 ± 0.03, and 1.78 ± 0.09 wt % water, respectively.

Luminescence Measurements. Luminescence measurements were made using a Cary Eclipse Fluorescence spectrophotometer (Varian Instruments, Walnut Creek, CA). Prior to any phosphorescence measurements, all samples were flushed for at least 15 min with nitrogen gas, which contained less than 1 ppm oxygen to eliminate oxygen quenching. At each target temperature, samples were equilibrated for 1 min/°C increase in temperature. The temperature was controlled using a thermo-electric temperature controller (Varian Instruments, Walnut Creek, CA). To eliminate moisture condensation during the measurements below room temperature, dry air was used to flush the chamber surrounding the cuvette holder. All of the measurements were made at least in triplicate.

Delayed fluorescence and phosphorescence emission spectra were collected from 520 to 750 nm (10 nm bandwidth) at 1 nm intervals using an excitation of 500 nm (20 nm bandwidth) over a temperature range from 5 to 100 °C with an observation window of 5.0 ms and an initial delay time of 0.2 ms, which suppresses fluorescence coincident with the lamp pulse. Emission spectra from sucrose or sucrose−starch films without probe were subtracted from each spectrum, although the signal of background was very low.

The energy of emission maximum (ν_p) and the full width at half-maximum (FWHM) of the emission bands were determined by using the log-normal line shape function[11] to fit both delayed fluorescence and phosphorescence.

$$I(\nu) = I_0 \exp\left\{-\ln(2)\left(\frac{\ln[1 + 2b(\nu - \nu_p)/\Delta]}{b}\right)^2\right\} \quad (1)$$

In eq 1, I_0 is the maximum emission intensity, ν_p is the peak frequency (cm^{-1}), Δ is a line width parameter, and b is an asymmetry parameter. This equation reduces to a Gaussian line width when $b = 0$. The bandwidth (FWHM; Γ) was calculated according to the following equation:

$$\Gamma = \Delta\left(\frac{\sinh(b)}{b}\right) \quad (2)$$

For delayed luminescence spectra collected from 520 to 750 nm, a sum of log-normal functions for delayed fluorescence ($I_{df}(\nu)$) and phosphorescence ($I_p(\nu)$) was used to fit the spectra. Each emission band was fit with independent parameters.

For lifetime measurements, samples were excited at 530 nm (20 nm bandwidth) and emission transients collected at 680 nm (20 nm bandwidth) over the temperature range from 5 to 100 °C. Phosphorescence intensity decays were collected over a window of 5 ms with an initial delay of 0.1 ms and increments of 0.04 ms. Each decay was the average of 20 cycles. Because intensity decays were nonexponential, a stretched exponential or Kohlrausch−Williams−Watts' decay function was selected to analyze the intensity decay.[11]

$$I(t) = I_0 \exp(-(t/\tau)^{\beta}) + \text{constant} \quad (3)$$

In eq 3, I_0 is the initial amplitude, τ is the stretched exponential lifetime, and β is an exponent varying from 0 to 1 that characterizes the distribution of lifetimes. The use of a stretched exponential model provides a direct measurement of a continuous distribution of lifetimes, which is appropriate for describing a complex glass possessing a distribution of relaxation times for the dynamic molecular processes. The smaller the β value, the more nonexponential the intensity decays and the broader the distribution of lifetimes. The program NFIT (Galveston, TX) was used to fit the decay; goodness of fit was evaluated by examining the values of χ^2 and R^2. Plots of modified residuals (defined as the difference between the intensity from the fit decay curve and the measured intensity divided by the square root of the measured intensity) were also used as an indicator of the goodness of fit. R^2 for all fits ranged from 0.99 to 1.00, and modified residual plots fluctuated randomly around zero amplitude.

Photophysical Scheme. Our analysis of the delayed emission is similar to the photophysical scheme for erythrosin B outlined by Duchowicz et al.[12] The measured emission rate for phosphorescence (k_P) is the sum of all possible de-excitation rates for the triplet state T_1:

$$\tau^{-1} = k_P = k_{RP} + k_{TS1} + k_{TS0} + k_Q[Q] \quad (4)$$

In this equation, k_{RP} is the rate of radiative emission to the ground state S_0; for erythrosin B, k_{RP} is 41 s^{-1} and constant with temperature.[12] The rate k_{TS1} is the rate of thermally activated reverse intersystem crossing from the triplet state T_1 to the singlet state S_1; its value can be estimated from the Arrhenius equation:

$$k_{TS1}(T) = k^0{}_{TS1} \exp(-\Delta E_{TS}/RT) \quad (5)$$

where k^0_{TS1} is the maximum rate of intersystem crossing from T_1 to S_1 at high temperature, ΔE_{TS} is the energy gap between T_1 and S_1, $R = 8.314$ J K^{-1} mol^{-1}, and T is the temperature in Kelvin. The value of ΔE_{TS} is calculated from the slope of a Van't Hoff plot of the natural logarithm of the ratio of intensity of delayed fluorescence (I_{DF}) to phosphorescence (I_P):

$$d[\ln(I_{DF}/I_P)]/d(1/T) = -\Delta E_{TS}/R \quad (6)$$

where I_{DF} and I_P are the maximum intensity values determined from an analysis of the emission band using eq 1. The value of k_{TS1} at 25 °C was estimated as 88 s^{-1} using $k^0_{TS1} = 3.0 \times 10^7$ s^{-1} and $\Delta E_{TS} = 31.56$ kJ/mol.[11]

In the presence of oxygen, the quenching rate $k_Q[Q]$ is the product of the rate constant k_Q and the oxygen concentration [Q]. By flushing nitrogen throughout the measurements, we assume that no oxygen quenching occurred. One of the nonradiative decay routes is through intersystem crossing to the ground state S_0. The decay rate is expressed by k_{TS0}, which reflects the rate of nonradiative quenching of the probe due to both internal and external factors. We assume that the term k_{TS0} primarily reflects the external environmental factors since the self-collisional quenching among probe molecules can be neglected within the extremely viscous amorphous solid. In this study, the temperature-dependent term k_{TS0} can be calculated from phosphorescence lifetime by rewriting eq 4.

$$k_{TS0}(T) = \frac{1}{\tau(T)} - k_{RP} - k_{TS1}(T) \quad (7)$$

Estimation of T_g of Sucrose/Starch Mixtures. The T_g values of the starch−sucrose mixtures were estimated using the following equation:

$$T_g = \frac{\sum_i w_i \Delta Cp_i T_{gi}}{\sum_i w_i \Delta Cp_i} \quad (8)$$

where w_i, ΔC_{pi}, and T_{gi} refer to the weight fraction, the change in specific heat capacity, and the glass transition temperature of individual components, respectively. T_g and ΔC_p for sucrose are 62 °C and 0.6 J/g °C, respectively.[13] For Hylon VII corn starch, T_g and ΔC_p were estimated on the basis of its composition (71% amylose and 29% amylopectin). We calculated T_g values of the mixtures using the values of T_g = 227 °C and ΔC_p= 0.49 J/g °C, which were reported by Orford et al.[14] when analyzing the DSC results of a series of saccharides ranging in DP from D-glucose up to amylose and amylopectin. Note, however, that the calculated T_g values of the starch−sucrose mixtures were not significantly affected by the choice of starch component T_g or ΔC_p values due to the very low starch contents of our samples.

RESULTS

At a probe/sucrose molar ratio of 1:10^4, each probe is on average surrounded by a matrix shell around 10−11 sucrose molecules thick; at this concentration, Ery B does not appear to aggregate within the matrix and thus reports the physical properties of the unperturbed sucrose matrix.

Delayed Emission Spectra. The delayed emission spectra of Ery B dispersed in amorphous sucrose films with various starch/sucrose weight ratios were collected over the temperature range from 5 to 100 °C. All spectra (data not shown) showed the typical decrease in phosphorescence and increase in delayed fluorescence intensity with increasing temperature exhibited by xanthene dyes. Both the delayed fluorescence and phosphorescence bands shifted to longer wavelength at higher temperature; the peak frequency (ν_p) and bandwidth (Γ) were determined by fitting to a log-normal line shape function (eqs 1 and 2). The effect of temperature on peak frequency and bandwidth for phosphorescence emission are plotted versus temperature in Figure 1. The peak frequency for delayed fluorescence exhibited similar behavior (data not shown).

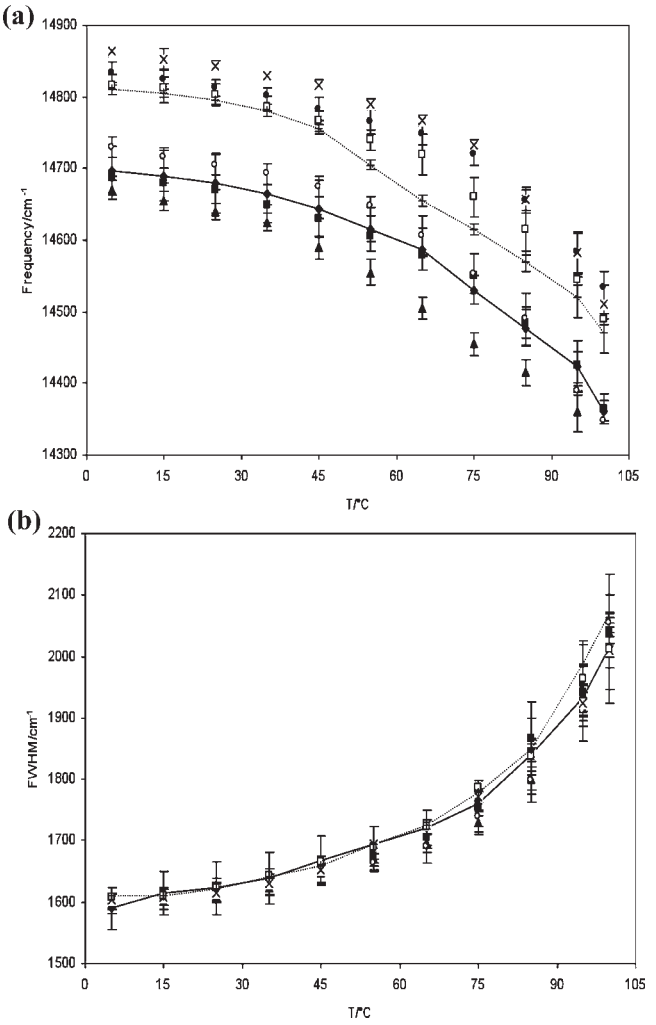

Figure 1. (a) Peak frequency (ν_p) and (b) bandwidth (full width at half-maximum, FWHM) for phosphorescence emission from erythrosin B in amorphous sucrose−starch films plotted as a function of temperature. Delayed emission spectra collected as a function of temperature were analyzed using the log-normal line shape function. Samples are erythrosin B in sucrose films with various starch/sucrose weight ratios (♦, control, 0; ■, 0.001; ▲, 0.0025; ○, 0.005; ×, 0.01; ●, 0.025; □, 0.05; +, 0.1).

The phosphorescence peak frequency provides a measure of the average energy of emission. The peak frequency decreased gradually and approximately linearly at low temperature and much more steeply at high temperature in all films. All curves had approximately the same temperature dependence. However, at a starch/sucrose wt ratio of 0.0025 the peak frequencies were below, while at a wt ratio higher than 0.005, the frequencies were above the values for pure sucrose. Addition of more starch decreased the peak frequency even further at both temperatures.

The total decrease in peak frequency ($\Delta\nu_p$) with changing temperature from 5 to 100 °C varied with starch content. Compared with sucrose ($\Delta\nu_p$ = 338 cm^{-1}), the decrease in peak frequency in starch/sucrose films was larger at low starch content but smaller at high starch content. With the addition of starch, $\Delta\nu_p$ increased to a maximum of 380 cm^{-1} at a wt ratio of 0.0025 and decreased to a minimum of 300 cm^{-1} at a wt ratio around 0.025.

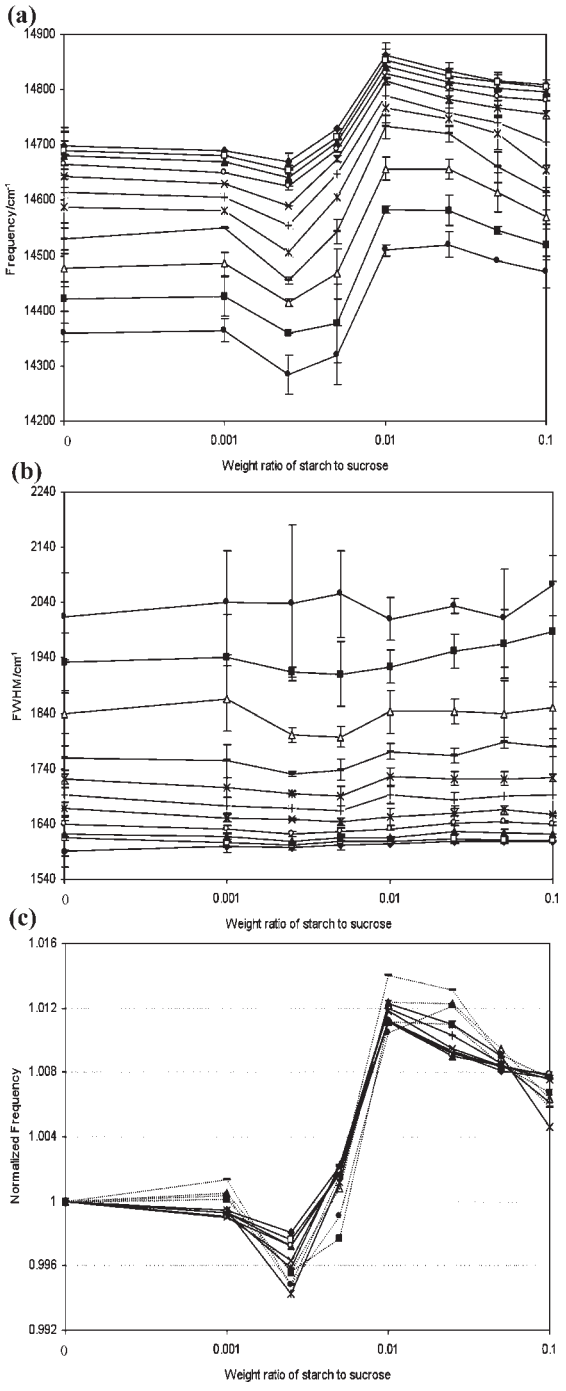

Figure 2. (a) Peak frequency (ν_p) and (b) bandwidth (full width at half-maximum, FWHM) for phosphorescence emission from erythrosin B in amorphous sucrose−starch films as a function of the weight ratio of starch/sucrose. (c) Peak frequency normalized at each temperature to the value in pure sucrose; for erythrosin B, phosphorescence in amorphous sucrose−starch films was plotted as a function of the weight ratio of starch/sucrose. Delayed emission spectra collected as a function of temperature were analyzed using the log-normal line shape function. From top to bottom, temperature increased from 5 to 100 °C with 10 °C increments (♦, 5 °C; □, 15 °C; ▲, 25 °C; ○, 35 °C; ×, 45 °C; +, 55 °C; *, 65 °C; −, 75 °C; Δ, 85 °C; ■, 95 °C; ●, 100 °C). In panel c, data below 65 °C are connected by a solid line and data above 65 °C by a dotted line.

The phosphorescence bandwidth is a measure of the extent of inhomogeneous broadening of the emission spectra. The bandwidth was essentially constant at ~1600 cm^{-1} at low temperature and increased gradually with low temperatures and more dramatically at high temperature in all films. The addition of starch did not significantly influence the bandwidth, and thus did not affect the extent of inhomogeneous broadening, over the whole temperature range.

The variation of the Ery B peak frequency and bandwidth with starch concentration are illustrated in Figure 2. The peak frequency varied in a complex fashion with starch content, decreasing to a minimum at wt ratio of 0.0025, increasing to a maximum at wt ratio 0.01, and then decreasing slightly at higher starch/sucrose wt ratios. In contrast, the bandwidth did not vary significantly with starch content. The effect of starch concentration is highlighted by the dependence of the normalized peak frequency (compared to the value in pure sucrose) on starch concentration at each temperature (Figure 2c).

The intensity ratio $\ln(I_{df}/I_p)$ was plotted as a van't Hoff plot versus $1/T$, and the slope obtained from the linear plot was used to estimate the energy gap (ΔE_{TS}) between the lowest triplet and singlet states (eq 6 in Materials and Methods). In amorphous sucrose, the value of ΔE_{TS} was 31.56 ± 0.56 kJ mol^{-1}. In the presence of starch with wt ratios of 0.001, 0.0025, 0.005, 0.01, 0.025, 0.05, and 0.1, the values of ΔE_{TS} were 31.92 ± 0.19, 31.32 ± 0.86, 31.64 ± 0.16, 32.12 ± 0.77, 31.13 ± 0.55, 31.32 ± 0.38, and 31.29 ± 0.16 kJ mol^{-1}, respectively, indicating that the addition of starch had no significant influence on the singlet−triplet energy gap.

Phosphorescence Intensity Decay Kinetics. The phosphorescence intensity decay of Ery B in sucrose−starch films with different starch contents was measured over the temperature range from 5 to 100 °C. All data were well-fit using a stretched exponential decay model.[11] The stretched exponential lifetime τ and stretching exponent β are plotted as a function of temperature in Figure 3. The lifetimes decreased gradually and linearly at low temperature and more dramatically at high temperature. The lifetime versus temperature curves were similar at all starch contents; however, the lifetimes at starch/sucrose wt ratios lower than 0.005 were smaller, while those with starch/sucrose wt ratios higher than 0.005 were larger than the lifetimes for pure sucrose at each temperature.

The stretching exponent, a measure of the width of the lifetime distribution in the amorphous matrix[11] also showed biphasic behavior over the temperature range from 5 to 100 °C; β was nearly constant at low temperature and decreased gradually at high temperature. The effect of starch on β varied with temperature: below ~65 °C, starch had little effect on β, whereas at higher temperature, starch decreased β below that in pure sucrose at low concentrations (<0.005 wt ratio) and increased β at higher concentrations. At high concentration, starch thus diminished the measured decrease in β at high temperature until, at wt ratio 0.01, β was nearly constant with temperature. The decrease in lifetime with temperature reflects an increase in the rate of nonradiative decay of the excited triplet T_1 state due to an increase in both the rate of nonradiative, matrix-induced decay to the ground state S_0 (k_{TS0}) and the rate of reverse intersystem crossing to S_1 (k_{TS1}). On the basis of the maximum physically reasonable value of k_{TS1},[11] an estimate of the lower limit of k_{TS0} was calculated using eq 7 (Materials and Methods). These values are plotted as $\ln(k_{TS0})$ versus $1/T$ in Figure 4. The matrix-induced quenching rate (k_{TS0}) was approximately constant at low temperature and increased significantly at high temperature. The increase in k_{TS0} occurred near the glass transition temperature, approximately 62 °C, in pure sucrose;[11] the temperature at which k_{TS0} increased was not significantly affected by the starch

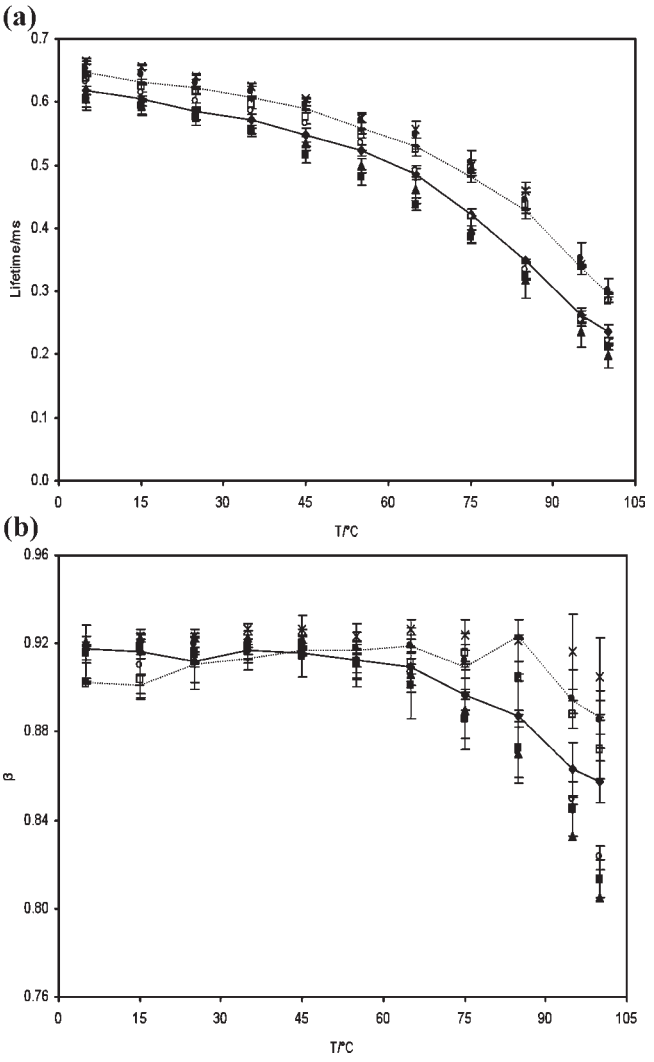

Figure 3. Temperature dependence of (a) lifetime and (b) stretching exponent β obtained from fits to a stretched exponential decay model of the intensity of decay of erythrosin B in amorphous sucrose films with various starch/sucrose weight ratios (♦, control, 0; ■, 0.001; ▲, 0.0025; ○, 0.005; ×, 0.01; ●, 0.025; □, 0.05; +, 0.1).

content of the films. The effect of starch on the matrix-induced quenching rate in sucrose is illustrated in Figure 5a in a plot of k_{TS0} versus wt ratio of starch at each temperature; k_{TS0} increased at low wt ratios of starch/sucrose and decreased at higher wt ratios. This trend is best illustrated in a plot of normalized k_{TS0} (normalized to the value in pure sucrose) plotted versus starch content (Figure 5b). At each temperature, k_{TS0} increased at low starch content, reaching a maximum value at wt ratio of 0.001−0.0025 and decreased below that of pure sucrose at higher wt ratio, reaching a minimum value at wt ratio 0.01, and then increased slightly to a plateau value at higher wt ratio. The effect of starch on k_{TS0} increased with temperature: compared to pure sucrose, k_{TS0} was 2% higher at 5 °C and 20% higher at 100 °C at a wt ratio of 0.001, and 6% lower at 5 °C and 17% lower at 100 °C at a wt ratio of 0.01.

DISCUSSION

Starch Conformation in Sucrose Films. The behavior of starch in solution is dependent on various factors, including the

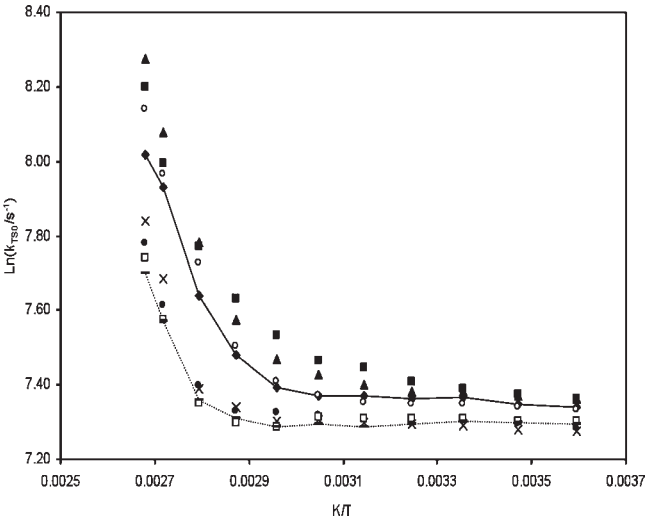

Figure 4. Arrhenius plot of the temperature effect on the rate constant for nonradiative decay of the triplet T_1 state to S_0 (k_{TS0}). Data were calculated from the lifetime data of Figure 3a; see text for additional details. Erythrosin B in amorphous sucrose films with various starch/sucrose weight ratios (♦, control, 0; ■, 0.001; ▲, 0.0025; ○, 0.005; ×, 0.01; ●, 0.025; □, 0.05; +, 0.1).

source of the starch, the amylose/amylopectin ratio, the presence of other components, and processing conditions (temperature, shear rate, and heating/cooling rate). Higher amylose content, for example, increases the gelatinization temperature, while sucrose inhibits granule swell, decreases the maximum viscosity, reduces the amount of soluble amylose from the granule, and enhances the gelatinization temperature through competition for water.[15] The gelatinization temperature of a 6% corn starch paste in the presence of 60% sucrose, for example, was reported as 100 °C compared to 60−70 °C in the absence of sucrose.[16]

In the present work, starch stock solutions at ∼3 wt % were prepared with vigorous stirring at temperature well above 100 °C before mixing with a concentrated sucrose solution. Upon gelatinization, amylose leached out of the granules adopts a random coil conformation at high temperature,[17] while amylopectin remains within the granules without any crystalline order.[18] Additional heating resulted in a continuous phase of solubilized amylose and amylopectin and a discontinuous phase of granule remnants, which were removed by microfiltration. We are thus confident that there were no crystalline or highly ordered granule-based structures present in the gelatinized starch−sucrose solution or in the films cast from this solution.

The solubilized components of gelatinized starch readily crystallize during retrogradation when cool. Sucrose is reported to prevent starch retrogradation,[19] and retrogradation does not occur at low water content.[18] Our sample preparation procedure involved the addition of gelatinized starch to a concentrated sucrose solution at temperatures close to 100 °C; then the mixture solution was kept at high temperature and filtered, rapidly spread, dried to a film under a heat gun, and stored in a desiccator at 0% RH for one week before data collection. We are thus confident that recrystallization of starch or formation of other orderly structures is negligible and that the starch molecules are dispersed as molecular species throughout the films.

A number of studies indicate that amylose molecules in neutral aqueous solution exhibit a global random coil conformation with locally helical segments.[17,20,21] This coil/helix conformation

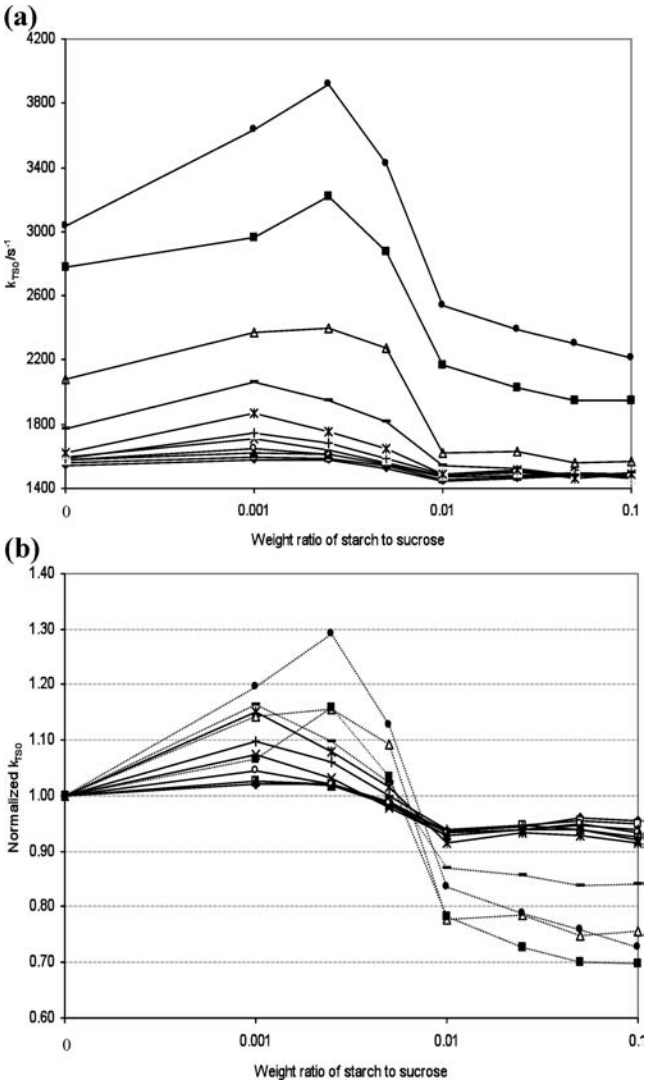

Figure 5. (a) Effect of starch on the rate constant for nonradiative decay of the triplet state to S_0 (k_{TS0}); data of Figure 4 were replotted as k_{TS0} versus the starch/sucrose weight ratio. (b) Normalized rate constant for nonradiative decay of the triplet state to S_0 (k_{TS0}) as a function of the starch/sucrose weight ratio at low starch contents. Data were collected at 5 °C (♦), 15 °C (□), 25 °C (▲), 35 °C (○), 45 °C (×), 55 °C (+), 65 °C (*), 75 °C (−), 85 °C (Δ), 95 °C (■), and 100 °C (●). In panel b, data below 65 °C are connected by a solid line and data above 65 °C by a dotted line.

seems common to amylose in a variety of solvents.[20] However, the locally ordered structure disappears at high water content and high temperature. Cheetham and Tao[22] found that the helical conformation decreased at high temperature with water content above 33%, and a complete transition from helix to coil was obtained at 66% water content. In the present study, gelatinization of starch in dilute aqueous solution ensures that the conformation of starch in solution is a uniformly random coil ($T_{gelatinization}$ > 63 °C, above which the amylose molecules must be in a random coil). Given that viscosity increases monotonically and dramatically due to drying during film formation, we expect that the starch macromolecules in the cast films maintain solution-like conformations. We thus conclude that our results provide insight into the effect of molecularly dispersed, random coil starch polymers on molecular mobility within the amorphous sucrose matrix.

Effect of Starch on the Mobility of Amorphous Sucrose. The phosphorescence emission wavelength and intensity of Ery B in amorphous sucrose and sucrose−starch mixtures are influenced by two kinds of molecular mobility: dipolar relaxation around the excited triplet state and matrix-induced, nonradiative quenching of the triplet state.[11] Our discussion of the effect of starch on molecular mobility in amorphous sucrose is based on an analysis of how the emission energy and lifetime data provide information about these two modes of molecular mobility.

The singlet−triplet energy gap ΔE_{TS} ($S_1 \leftarrow T_1$), determined from thermal activation of delayed fluorescence, was essentially identical at all starch concentrations, suggesting that the presence of starch in the sucrose matrix did not directly modulate the energy of the triplet state. The peak emission energy, however, a measure of the ($S_0 \leftarrow T_1$) energy gap, reflects the extent of dipolar relaxation around the excited triplet state prior to emission; a decrease in the peak energy thus reflects an increase in the ratio of the dipolar relaxation rate to the emission rate (k_P), while an increase in energy reflects a decrease in this ratio. The peak emission energy varied with the amount of starch, decreasing slightly at low (<0.005 wt ratio) starch content, increasing significantly at intermediate (~0.01 wt ratio) starch content, and then decreasing slightly at higher starch content; the ratio of dipolar relaxation rate/emission rate thus increased, decreased, then increased again as starch content increased. Given that the emission rate increased at low starch content and decreased at higher starch content (see below), these data suggest that starch caused an increase in dipolar relaxation rate at low starch content and a decrease at higher starch contents. This direct effect of mobility on the peak energy may be modulated at the highest starch content by a decrease in overall matrix polarity due to the lower average density of polar hydroxyl groups in starch (3 per monomer of 162 g mol^{-1} or 0.019/g) versus sucrose (8 per molecule of 342 g mol^{-1} or 0.023/g).

The emission intensity and the lifetime are directly modulated by the rates of radiative emission (k_{RP}), of reverse intersystem crossing to the excited triplet state (k_{TS1}), and of intersystem crossing to the ground state (k_{TS0}). The rate of nonradiative quenching, k_{TS0}, which is modulated by the physical state of the amorphous matrix, reflects both the manner in which the excited T_1 state is vibrationally coupled to the S_0 ground state as well as the manner in which the ground state vibrational energy can be dissipated from the excited probe into the surrounding matrix; since the efficiency of this vibrational dissipation is related to the overall mobility of the matrix, k_{TS0} provides a measure of matrix mobility.[23,11] The variation of the Ery B lifetime with starch content indicated that k_{TS0}, and thus matrix molecular mobility, increased at low (<0.005 wt ratio) and decreased at higher starch content to a plateau value at a wt ratio of 0.01 and above.

Two distinct spectroscopic signals from Ery B thus indicate that starch increases mobility at low starch content and decreases mobility at high starch content. We interpret these effects of starch in terms of its complex influence on the integrity and connectivity of the hydrogen-bonded network within the sucrose matrix. On the one hand, steric and geometric constraints on starch hydroxyls may inhibit their ability to form strong, well ordered hydrogen bonds with sucrose hydroxyls, thus weakening the hydrogen-bonded network, perhaps increasing the free volume, and thus increasing matrix molecular mobility. On the other hand, individual starch molecules can hydrogen bond to a large number of sucrose molecules widely distributed throughout the matrix; this continuous starch−sucrose network and, at

sufficiently high starch concentration, starch−starch network, can dynamically couple large regions of the matrix, and thus decrease molecular mobility. Our results suggest that local constraints on hydrogen bonding dominate at low starch concentration and large-scale effects on dynamic coupling dominate at high starch concentration.

The mobility of the sucrose matrix is measurably increased at 0.001 wt ratio of starch; at this concentration, ∼475 sucrose molecules, or a shell ∼22 molecules thick, are perturbed by each glucose monomer along the starch polymer. The corn starch Hylon VII used in this study is 71% amylose with the molecular weight ranging from 243,000 to 972,000, while the remaining amylopectin has a highly branched structure with a molecular weight ranging from 10^6-10^9 g mol^{-1}. If we assume that the bulk of the dynamic effect is due to amylose, given its much more extended conformation, then the mobility of the sucrose matrix is measurably affected at a starch/sucrose mole ratio of $\sim 4 \times 10^{-7}$. At 0.01 wt ratio starch, where the matrix mobility is decreased the most, ∼48 sucrose molecules are dynamically perturbed by each glucose monomer or a solvent shell ∼7 molecules thick along the polymer. Again, assuming that the effect is due to amylose, the maximum decrease occurs at a starch/sucrose mole ratio of $\sim 4 \times 10^{-6}$. Including amylopectin in the analysis gives measurable effects at even lower starch/sucrose mole ratios (due to the large size of the amylopection.)

The propagation of dynamic effects over extended regions argues for enormous cooperativity in the dynamic behavior of the amorphous sucrose matrix. Our confidence in effects at these low concentrations is bolstered by our previous studies of the effect of gelatin[24] and xanthan gum[25] on sucrose molecular mobility using Ery B phosphorescence; these studies found a remarkably similar dependence of matrix mobility on polymer concentration. Both carbohydrate and protein polymers are thus able to perturb the sucrose matrix at extremely low mole ratios.

The residual water content of the films increased with starch content from 0.56 ± 0.13 wt % in pure sucrose to 1.78 ± 0.09 wt % in films with starch wt ratios of 0.1 (see Materials and Methods). This increase in residual water, albeit small, may affect the matrix mobility at higher starch concentrations in complex ways.

Influence of Starch on Dynamic Site Heterogeneity. Supercooled liquids and amorphous polymers are known from a range of techniques to be dynamically heterogeneous both through space at any given time and through time at any given place.[26] Spectral heterogeneity of Ery B phosphorescence consistent with dynamic site heterogeneity has been observed in a variety of amorphous sugars and sugar alcohols[11,27] and proteins,[28] indicating that such dynamic heterogeneity may be a characteristic feature of amorphous biomaterials.

The temperature dependence of the stretching exponent β indicates that the values of β in the glassy sucrose−starch films were slightly larger at low starch contents but significantly smaller at high starch contents, suggesting that small amounts of starch slightly decreased the matrix heterogeneity while large amounts of starch increased heterogeneity in the glassy state. The effect of starch on spectroscopic heterogeneity was sensitive to temperature. At high temperature, starch increased heterogeneity at low starch content but reduced heterogeneity at high concentration.

The emission bandwidth decreased slightly with the addition of starch, indicating a decrease in the width of the distribution of energetically distinct matrix environments both in the glass and in the melt. However, at high starch/sucrose ratios, the bandwidth increased slightly at high temperature.

These spectroscopic characteristics thus suggest that the addition of a small amount of starch caused perhaps a small decrease in dynamic heterogeneity, while higher concentrations increased dynamic heterogeneity in amorphous sucrose.

Amorphous sucrose is considered structurally heterogeneous and appears to organize into sucrose clusters.[29] Pure sucrose glass also has dynamically distinct sites with varied emission energy and matrix quenching rate.[11] Although an increase in heterogeneity is expected at high starch contents, even a small decrease in heterogeneity at low concentration is unexpected in a mixture. Poirier-Brulez et al.[10] found similar results when they investigated the sucrose effect on mobility in starch-based glasses. The relaxation time distribution indicator β was larger (and thus less heterogeneous) in starch glass mixed with sucrose (0.56) than in pure starch (0.31) or in pure sucrose (0.32, reported by Urbani et al.;[30] or 0.51, reported by Hancock et al.[31]). They proposed that the larger value was probably a sign of an asymmetric distribution dominated by short times through a narrow peak over a wide basis at larger relaxation time values. Such an explanation may apply to our results.

Effect of Starch on Sucrose Glass Transition Temperature. The addition of starch did not significantly increase the T_g of the sucrose matrix in the studied concentration range. The estimated T_g values for starch−sucrose mixtures at ratios less than 0.025 varied between 62 and 63 °C (compared with 62 °C for pure sucrose). At a ratio of 0.05, the calculated T_g value increased to 68 °C. Note that starch−sucrose amorphous films contain residual water varying from 0.5 to 1.8%. As a plasticizer, water decreased the T_g and increased the flexibility and mobility of films, which counteracted the effect of starch on T_g. If residue water was considered, the calculated T_g value for sucrose decreased to 60 °C, and the values for starch−sucrose mixtures at ratios below 0.05 were almost the same as the T_g for sucrose. At a ratio of 0.05, the value increased to 62 °C. These calculations provide evidence that starch affects sucrose matrix mobility primarily by modulating local mobility motions through specific intermolecular interactions rather than by modulating the glass transition temperature that reflects the main chain movement.

We estimated temperatures for a transition in molecular mobility from the intersection of linear trendlines in Arrhenius plots of k_{TS0} at high and low temperatures. The calculated transition temperatures were 76.5 °C in sucrose and 74.4, 74.7, 73.3, 83.0, 83.2, 84.4, and 83.7 °C in the sucrose−starch mixtures with starch/sucrose wt ratios of 0.001, 0.0025, 0.005, 0.01, 0.025, 0.05, and 0.1, respectively. The trend in these values, a small decrease in transition temperature at low starch contents and a significant increase at high starch contents, reflects the trend seen in all other mobility data reported here. All of these spectroscopic data indicate that the addition of starch increased mobility in the sucrose matrix at low concentration while keeping the probe in a rigid environment over a wider temperature range at higher starch content.

AUTHOR INFORMATION

Corresponding Author
*E-mail: ludescher@aesop.rutgers.edu.

ABBREVIATIONS

Ery B, erythrosin B; FWHM, full width at half-maximum; T_g, glass transition temperature.

REFERENCES

(1) Chang, L.; Shepherd, D.; Sun, J.; Ouellette, D.; Grant, K. L.; Tang, X.; Pikal, M. J. Mechanisms of protein stabilization by sugars during freeze-drying and storage: native structure preservation, specific interaction, and/or immobilization in a glassy matrix? *J. Pharm. Sci.* **2005**, *94* (7), 1427–1444.

(2) Kets, E. P. W.; IJpelaar, P. J.; Hoekstra, F. A.; Vromans, V. Citrate increases glass transition temperature of vitrified sucrose preparations. *Cryobiology* **2004**, *48*, 46–54.

(3) Franks, F.; Hatley, R. H. M.; Mathias, S. F. Materials science and the production of shelf-stable biologicals. *Pharm. Technol. Int.* **1991**, 3, 24–34.

(4) Crowe, J. H.; Crowe, L. M.; Carpenter, J. F. Preserving dry biomaterials: the water replacement hypothesis. Part 1. *BioPharm.* **1993**, *6*, 28−29, 32–33.

(5) Allison, S. D.; Manning, M. C.; Randolph, T. W.; Middleton, K.; Davis, A.; Carpenter, J. F. Optimization of storage stability of lyophilized actin using combinations of disaccharides and dextran. *J. Pharm. Sci.* **2000**, *89*, 199–214.

(6) Benczedi, D.; Tomka, L.; Escher, F. Thermodynamics of amorphous starch-water systems. 1. Volume fluctuations. *Macromolecules* **1998**, *31*, 3055–3061.

(7) Partanen, R.; Marie, V.; MacNaughtan, W.; Forssell, P.; Farhat, I. ^{1}H NMR study of amylose films plasticized by glycerol and water. *Carbohydr. Polym.* **2004**, *56*, 147–155.

(8) Gaudin, S.; Lourdin, D.; Le Botlan, D.; Ilari, J. L.; Colonna, P. Plasticization and mobility in starch-sorbitol films. *J. Cereal Sci.* **1999**, *29*, 273–284.

(9) Lourdin, D.; Bizot, H.; Colonna, P. Antiplasticization in starch-glycerol films? *J. Appl. Polym. Sci.* **1997**, *63*, 1047–1053.

(10) Poirier-Brulez, F.; Roudaut, G.; Champion, D.; Tanguy, M.; Simatos, D. Influence of sucrose and water content on molecular mobility in starch-based glasses as assessed through structure and secondary relaxation. *Biopolymers* **2006**, *81*, 63–73.

(11) Pravinata, L. C.; You, Y.; Ludescher, R. D. Erythrosin B phosphorescence monitors molecularmobility and dynamic site heterogeneity in amorphous sucrose. *Biophys. J.* **2005**, *88* (May), 3551–3561.

(12) Duchowicz, R.; Ferrer, M. L.; Acuna, A. U. Kinetic spectroscopy of erythrosin phosphorescence and delayed fluorescence in aqueous solution at room temperature. *Photochem. Photobiol.* **1998**, *68*, 494–501.

(13) Roos, Y. *Phase Transitions in Foods*; Academic Press: San Diego, CA, 1995.

(14) Orford, P. D.; Parker, R.; Ring, S. G.; Smith, A. C. Effect of water as a diluent on the glass transition behaviour of malto-oligosaccharides, amylose and amylopectin. *Int. J. Biol. Macromol.* **1989**, *11*, 91–96.

(15) Savage, H. L.; Osman, E. M. Effects of certain sugars and sugar alcohols on the swelling of corn starch granules. *Cereal Chem.* **1978**, *55*, 447–454.

(16) Zallie, P. J. The role and function of specialty starches in the confection industry. *Mfg. Confect.* **1988**, November.

(17) Hayashi, A.; Kinoshita, K.; Miyake, Y. Conformation of amylose in solution. *Polym. J. (Tokyo, Jpn.)* **1981**, *13* (6), 537–541.

(18) Eliasson, A. *Carbohydrates in Food*, 2nd ed.; Taylor & Francis: New York, 2006.

(19) Le Botlan, D.; Desbois, P. Starch retrogradation study in presence of sucrose by low-resolution nuclear magnetic resonance. *Cereal Chem.* **1995**, *72* (20), 191–193.

(20) Norisuye, T. Viscosity behavior and conformation of amylose in various solvents. *Polym. J. (Tokyo, Jpn.)* **1994**, *26* (11), 1303–1307.

(21) Norisuye, T. Conformation and properties of amylose in dilute solution. *Food Hydrocolloids* **1996**, *10* (1), 109–115.

(22) Cheetham, N. W. H.; Tao, L. Amylose conformational transitions in binary DMSO/water mixtures. *Starch/Staerke* **1997**, *49* (10), 407–415.

(23) Fischer, C. J.; Gafni, A.; Steele, D. G.; Schauerte, J. A. The triplet state lifetime of indole in aqueous and viscous environments. *J. Am. Chem. Soc.* **2002**, *124*, 10359–10366.

(24) You, Y.; Ludescher, R. D. Effect of gelatin on molecular mobility in amorphous sucrose detected by erythrosin B phosphorescence. *Carbohydr. Res.* **2008**, *343*, 2657–2666.

(25) You, Y; Ludescher, R. D. Effect of xanthan on the molecular mobility of amorphous sucrose detected by erythrosin B phosphorescence. *J. Agric. Food Chem.* **2009**, *57*, 709–716.

(26) Richert, R. Heterogeneous dynamics in liquids: fluctuations in space and time. *J. Phys.: Condens. Matter* **2002**, *14*, R738–R803.

(27) Shirke, S.; Ludescher, R. D. Dynamic site heterogeneity in amorphous maltose and maltitol from spectral heterogeneity in erythrosin B phosphorescence. *Carbohydr. Res.* **2005**, *340*, 2661–2669.

(28) Nack, T. J.; Ludescher, R. D. Molecular mobility and oxygen permeability in amorphous bovine serum albumin films. *Food Biophys.* **2006**, *1*, 151–162.

(29) Molinero, V.; Cagin, T.; Goddard, W. A., III. Sugar, water and free volume networks in concentrated sucrose solutions. *Chem. Phys. Lett.* **2003**, *377*, 469–474.

(30) Urbani, R.; Sussich, F.; Prejac, S.; Cesaro, A. Enthalpy relaxation and glass transition behaviour of sucrose by static and dynamic DSC. *Thermochim. Acta* **1997**, *304*−*305*, 359–367.

(31) Hancock, B. C.; Shamblin, S. L.; Zografi, G. Molecular mobility of amorphous pharmaceutical solids below their glass transition temperatures. *Pharm. Res.* **1995**, *12* (6), 799–806.